

Electronic structure and magnetic properties of high-spin octahedral Co(II) complexes: Co(II)(acac)₂(H₂O)₂

Lawrence L. Lohr, Jeremy C. Miller, and Robert R. Sharp
Department of Chemistry, University of Michigan, Ann Arbor, Michigan 48109-1055

(Received 29 June 1999; accepted 16 September 1999)

An analysis of the electronic structure of the high-spin $3d^7$ Co(II) ion in the approximately octahedral Co(II)(acac)₂(H₂O)₂ complex is presented in terms of crystal fields of descending symmetry from octahedral to orthorhombic. The energies and wave functions resulting from the interplay of these fields with the spin-orbit coupling are used to obtain zero-field splittings, magnetic moments, magnetic susceptibilities, and g values for the complex. The calculated temperature dependence of the susceptibility is compared to the reported dependence for Co(II)(acac)₂(H₂O)₂, yielding bounds on the strength of the tetragonal component of the crystal field. The calculated anisotropy in the susceptibility is used in an analysis of our observed pseudocontact NMR shifts for methyl and methine protons in the complex. A procedure is outlined for using a crystal field analysis to compute pseudocontact contributions to proton chemical shifts starting from g values extracted from ESR spectra. The relationship between molecular structure and crystal-field splittings is also explored via a series of *ab initio* electronic structure calculations for the M(II)(acac)₂(H₂O)₂ complexes with M=Mn, Co, Ni, and Zn. © 1999 American Institute of Physics. [S0021-9606(99)01446-4]

INTRODUCTION

We have recently published^{1,2} a series of experimental and theoretical studies of proton NMR relaxation in paramagnetic transition metal complexes. The first¹ of these focused on the $S=1$ complex *trans*-Ni(II)(acac)₂(H₂O)₂, where “acac” denotes the acetylacetonate anion. We presented a molecular-frame theoretical model appropriate to this complex, in which the zero-field splitting (ZFS) of the electronic spin triplet is larger than the electronic Zeeman energy, with the result that the electron spin precessional motion is spatially quantized with respect to the molecule-fixed principal axis system of the orthorhombic ZFS tensor of this D_{2h} symmetry complex. The proton NMR relaxation enhancement R_{1p} was shown to arise from additive molecular-frame Cartesian components of the time-dependent electron spin magnetic moment operator $\mu(t)$. The second of our studies² focused on the $S=2$ complex Mn(III)-TPPS, where “TPP” denotes the tetraphenylporphyrin dianion and “S” the sulfonate anion. The high-spin Mn(III) ion has an orbitally degenerate 5E_g ground term if octahedral, with the result that the ZFS for this ion in its tetragonal site (D_{4h} symmetry) in the TPPS complex is quite large. We analyzed the observed magnetic field dependence of the proton NMR relaxation in terms of a field-dependent quantization of the electron spin states arising from the 5E_g ground term.

Crystal-field (or ligand-field) analyses involving the interplay of spin-orbit coupling and low-symmetry crystal fields were an important part of the theoretical part of our studies of proton NMR relaxation in both the Ni(II) and Mn(III) systems described above. The next paramagnetic system which we have studied experimentally and theoretically is the complex *trans*-Co(II)(acac)₂(H₂O)₂, similar to

the corresponding Ni(II) complex, but containing instead the high-spin ($S=3/2$) $3d^7$ Co(II) ion. This ion is an orbitally degenerate $^4T_{1g}$ ground term if octahedral, with the result that it is subject to a first-order spin-orbit splitting. The magnetic behavior of this *bis*-acac Co(II) complex was carefully studied³ as a function of temperature by Figgis *et al.*, who measured the magnetic susceptibility of this and 14 other high-spin Co(II) complexes in the range 78–295 K. An extended crystal-field model of the $^4T_{1g}$ ground term was employed to analyze the data, leading to a value of the effective magnetic moment of 4.96 B.M. (Bohr magnetons) at 295 K for the *bis*-acac complex. In our present study we utilize a closely related model to obtain the zero-field splitting tensor, the g tensor, and the magnetic susceptibility tensor for the *trans*-Co(II)(acac)₂(H₂O)₂ complex. These results are used here in an analysis of the pseudocontact proton NMR shift in this complex and will also be used in an analysis to be published later of proton NMR relaxation mechanisms in this and other high-spin Co(II) complexes. We also explore the relationship between molecular structure and crystal-field splittings for this complex via a series of *ab initio* electronic structure calculations for the M(II)(acac)₂(H₂O)₂ complexes with M=Mn, Co, Ni, and Zn.

To the extent that only the lowest Kramers' doublet for a high-spin Co(II) complex is thermally populated the anisotropy in the magnetic susceptibility tensor is simply related to the anisotropy in the g tensor, the latter obtainable in favorable cases from ESR spectra. The relationship between these properties provides an experimental basis for determining the susceptibility component values which are needed for the interpretation of nmr hyperfine chemical shifts.

OCTAHEDRAL CRYSTAL FIELDS

The Co(II) ion in the approximately octahedral Co(II)(acac)₂(H₂O)₂ complex is a high-spin $3d^7$ ion. We describe its electronic structure in terms of magnetic moments, magnetic susceptibilities, and g values via a series of approximations associated with descending symmetry, beginning here with octahedral crystal fields. Throughout our analysis we shall primarily use the parameters employed by Figgis *et al.* in their fit³ of the temperature dependence of the magnetic susceptibility of this complex. These parameters are 9300 cm⁻¹ for the octahedral splitting Δ , 980 cm⁻¹ for the electron–electron repulsion parameter B , 510 cm⁻¹ for the free-ion spin–orbit parameter ζ_0 , and 435 cm⁻¹ for the free-ion spin–orbit parameter ζ in the complex. Values for the parameters describing the crystal-field splittings in tetragonal and orthorhombic symmetries are given in later sections.

The $3d^7$ configuration gives rise to two high-spin ($S = 3/2$) multiplets, namely the lower energy 4F and the higher energy 4P . Under the influence of an octahedral crystal field the 4F multiplet splits, in ascending energy order, into $^4T_{1g}$, $^4T_{2g}$, and $^4A_{2g}$ multiplets, while 4P transforms as $^4T_{1g}$. In addition the octahedral field mixes the two $^4T_{1g}$ multiplets. We choose the alternative description in which the pair of $^4T_{1g}$ multiplets are associated with the strong-field configurations $t_{2g}^5 e_g^2$ and $t_{2g}^4 e_g^3$; this description in no way implies that the octahedral splitting parameter Δ (or $10 Dq$) is necessarily large. In this strong-field basis the 2×2 matrix \mathbf{H} of the octahedral crystal field and the electron–electron repulsion is given⁴ by

$$\mathbf{H} = \begin{pmatrix} \Delta + 9B & -6B \\ -6B & 0 \end{pmatrix} \quad (1)$$

in which the $t_{2g}^5 e_g^2$ diagonal element is arbitrarily set to zero. Each two-component eigenvector may be written in the form

$$\psi = \cos \alpha |t_{2g}^5 ({}^2T_{2g}) e_g^2 ({}^3A_{2g}) {}^4T_{1g}\rangle + \sin \alpha |t_{2g}^4 ({}^3T_{1g}) e_g^3 ({}^2E_g) {}^4T_{1g}\rangle. \quad (2)$$

The effective orbital angular momentum of a given $^4T_{1g}$ multiplet may be written as $\gamma \mathbf{L}$, where γ is given in terms of the coefficients in Eq. (2) by

$$\gamma = -\cos^2 \alpha - 2 \sin \alpha \cos \alpha + (1/2) \sin^2 \alpha. \quad (3)$$

The orbital angular momentum operator \mathbf{L} is taken to operate on an $L=1$ pseudo- P effective multiplet. As discussed by Griffith,⁵ $-3/2 \leq \gamma \leq -1$, with $\gamma \rightarrow -3/2$ in the weak-field limit ($\alpha \rightarrow \pi/2$) and $\gamma \rightarrow -1$ in the strong-field limit ($\alpha \rightarrow 0$). Taking the electron–electron repulsion parameter B to have the value 980 cm⁻¹, γ for the lower-energy $^4T_{1g}$ multiplet has values of -1.469 , -1.416 , and -1.365 for Δ values of 5000, 10 000, and 15 000 cm⁻¹, respectively. The value of γ is close to -1 only for very large Δ values ($\gamma = -1.181$ for $\Delta = 50\,000$ cm⁻¹), for which the Co(II) complex would be low spin anyway. Throughout the remainder of this paper we use a value of $\gamma = -1.424$ corresponding to $\Delta = 9300$ cm⁻¹.

We next calculate the eigenvalues and eigenvectors of the matrix of the effective spin–orbit operator $H_{so} =$

$-(1/3) \gamma \zeta \mathbf{L} \cdot \mathbf{S}$ calculated with respect to the 12-component basis $|M_S M_L\rangle$ for the lower-energy $^4T_{1g}$ multiplet. Since γ is negative, the first-order splitting of the $^4T_{1g}$ multiplet follow a normal Landé ordering, with energies of $(5/6) \gamma \zeta$, $(1/3) \gamma \zeta$, and $-(1/2) \gamma \zeta$ for levels with $J=1/2$, $3/2$, and $5/2$, respectively. These levels may be assigned octahedral double-group labels E'_g , U'_g , and $E''_g + U'_g$ if desired, although the sixfold degeneracy associated with $J=5/2$ is retained to first order. Taking γ as -1.424 (Δ as 9300 cm⁻¹) and using the Co(II) free-ion value of 435 cm⁻¹ for the spin–orbit parameter ζ_0 , the $J=3/2$ and $J=5/2$ levels lie at energies of 310 cm⁻¹ (445 K) and 826 cm⁻¹ (1188 K) above the $J=1/2$ ground level.

We next incorporate these energies into Griffith's expressions⁵ for the magnetic susceptibility X of an octahedral high-spin d^7 complex in terms of an effective Bohr magneton number μ_{eff} . These expressions, adapted to SI units so that X is the molar susceptibility in m³ mol⁻¹, are

$$X = (\mu_0 N_0 \beta^2 / 3kT) \sum W_J \mu_{\text{eff}}^2(J) / \sum W_J, \quad (4a)$$

$$\mu_{\text{eff}}^2(1/2) = (5 g_e / 2 - \gamma)^2 / 3 - 20(g_e - \gamma)^2 / 3x \gamma, \quad (4b)$$

$$\mu_{\text{eff}}^2(3/2) = (11 g_e / 2 + 2 \gamma)^2 / 15 + 88(g_e - \gamma)^2 / 75x \gamma, \quad (4c)$$

$$\mu_{\text{eff}}^2(5/2) = 7(3 g_e / 2 + \gamma)^2 / 5 + 36(g_e - \gamma)^2 / 25x \gamma, \quad (4d)$$

where the W_J are Boltzmann factors including the level degeneracy $2J+1$, x is ζ/kT , μ_0 is the vacuum permeability, N_0 is Avogadro's number, k is the Boltzmann constant, β is the Bohr magneton (B.M.), g_e is the free-electron g value 2.0023, and the summation is over J . The first term in each $\mu_{\text{eff}}^2(J)$ expression is independent of the temperature T and hence gives rise to a $1/T$ first-order contribution to X , while the second term, proportion to T , gives rise to a temperature-independent second-order contribution to X . The resulting value of the susceptibility X may be applied to deformed octahedral d^7 complexes if we invoke Van Vleck's theorem⁶ that low-symmetry crystal fields do not affect the magnetic susceptibility to first-order. We obtain a thermally averaged rms μ_{eff} value of 5.14 B.M. at 298 K, essentially identical to the value of 5.11 B.M. extracted by Abernathy⁷ from the room temperature magnetic susceptibility of a powdered Co(II)(acac)₂(H₂O)₂ sample, but slightly higher than the value of 4.96 B.M. at 295 K measured³ by Figgis *et al.* If our calculation is restricted to the lowest three doublets the value is only slightly larger, namely 5.25 B.M., but if restricted to the lowest doublet it is much too large, namely 6.32 B.M., thus indicating the importance of the $J=3/2$ level, but not the $J=5/2$ level, for the susceptibility at 298 K. The range of applicability of Van Vleck's theorem to our Co(II) complex is discussed in the section on Magnetic Moments in Low-Symmetry Crystal Fields, in which we show that consideration of the tetragonal field does bring our calculated magnetic moment into very close agreement with the value of Figgis *et al.*, but that the smaller orthorhombic field does not significantly affect the computed moment.

TETRAGONAL CRYSTAL FIELDS

Our next step is to consider the effect of a tetragonal crystal field simultaneously with the spin-orbit coupling and then to calculate g values separately for each thermally populated Kramers' doublet. The environment about the Co(II) ion in the Co(II)(acac)₂(H₂O)₂ complex is actually of only D_{2h} symmetry, but we idealize this to D_{4h} symmetry for present purposes. From an x-ray structure⁸ the Co-O distances in the Co(II)(acac)₂(H₂O)₂ complex to the four acac O atoms average 2.04 Å, while those to the two water O atoms average 2.22 Å, thus approximating a tetragonally elongated complex with D_{4h} symmetry. The effect of such an axial field on a $^4T_{1g}$ multiplet may be expressed⁵ by the effective Hamiltonian H_{ax} , where

$$H_{ax} = -\delta(L_z^2 - 2/3). \quad (5)$$

As with the previously defined orbital magnetic moment and spin-orbit Hamiltonian operators, the operand is taken as an $L=1$ pseudo- P multiplet. Positive δ corresponds to a splitting with 4E_g below $^4A_{2g}$, and is associated with an axial compression, while negative δ corresponds to a splitting with $^4A_{2g}$ below 4E_g , and is associated with an axial elongation, as in our Co(II)(acac)₂(H₂O)₂ complex. (Our parameter δ corresponds in magnitude to the axial splitting parameter " Δ " of Figgis *et al.*, but is given an opposite sign convention.) To the extent that the lower energy $^4T_{1g}$ multiplet derives exclusively from the strong-field configuration $t_{2g}^5e_g^2$ the axial splitting parameter δ represents the comparatively small separation between the (xz, yz) pair of t_{2g} orbitals and the xy t_{2g} orbital. (For $\Delta=9\,300\text{ cm}^{-1}$, the fraction of this configuration is 0.919.) The comparatively large separation of the $3z^2-r^2$ and x^2-y^2 e_g orbitals contributes to the axial splitting of a $^4T_{1g}$ multiplet only to the extent that the configuration $t_{2g}^4e_g^3$ contributes.

Griffith has tabulated⁹ the matrices of the spin-orbit coupling H_{so} and axial crystal field H_{ax} Hamiltonians with respect to the six Kramers' spin-orbit doublets arising from a $^4T_{1g}$ multiplet. These matrices are of size 3×3 for $|M_J|=1/2$, 2×2 for $|M_J|=3/2$, and 1×1 for $|M_J|=5/2$. We take $\delta < 0$, so that the lowest energy eigenvector of the $|M_J|=1/2$ matrix and the lower energy eigenvector of the $|M_J|=3/2$ matrix correspond to the two doublets arising from the $^4A_{2g}$ multiplet. After diagonalizing these matrices, we calculate electronic magnetic moments, to which g values are proportional, by assuming that all Zeeman energies are small compared to the zero-field splittings between Kramers' doublets produced by the interplay of the spin-orbit coupling and the tetragonal crystal fields. That is, we consider Zeeman interactions within each Kramers' pair but ignore interactions between pairs. This treatment constitutes first-order degenerate Zeeman perturbation theory, leading to a 2×2 Zeeman matrix for each doublet; the eigenvalues for a given direction of the magnetic induction \mathbf{B} with respect to the molecular axes yield the appropriate magnetic moments as Zeeman energy eigenvalues per unit of magnetic induction. The magnetic moment operator μ is taken as $\beta(\gamma\mathbf{L} + g_e\mathbf{S})$, where g_e is the free-electron g value 2.0023. From the eigenvalues μ_{kk} of each magnetic moment matrix, g_{kk} values are

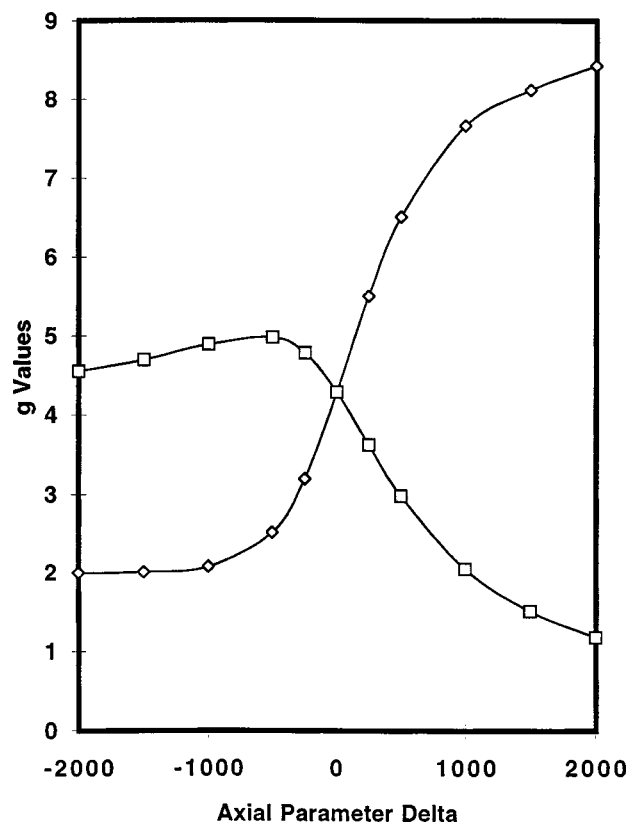


FIG. 1. Dependence of $g_{xx}=g_{\perp}$ (□) and $g_{zz}=g_{\parallel}$ (◇) values for the lowest Kramers' doublet of high-spin Co(II) on the axial splitting parameter δ in cm^{-1} , with all values referenced to $S'=1/2$ and computed using $\gamma=1.424$ ($\Delta=9300\text{ cm}^{-1}$) and $\zeta=435\text{ cm}^{-1}$. Negative δ corresponds to axial elongation, positive to axial compression.

obtained, assuming a reference effective spin $S'=1/2$, by $g_{kk}=2\mu_{kk}/\beta$, where $k=x, y$, and z denote molecular axes. Note that the μ_{kk} values do not correspond to the μ_{eff} values described in the section on octahedral crystal fields, as the μ_{eff} include the excited-state contributions associated with temperature-independent paramagnetism, while the μ_{kk} do not.

The axially symmetric tetragonal case is special in that the 2×2 Zeeman matrices for each doublet are diagonal in the basis $|M_S M_L\rangle$ for $\mathbf{B}\parallel z$, but purely off-diagonal for $\mathbf{B}\perp z$. Taking as before $\gamma=-1.424$ ($\Delta=9\,300\text{ cm}^{-1}$) and $\zeta=435\text{ cm}^{-1}$, together with $\delta=-550\text{ cm}^{-1}$, we obtain for the $|M_J|=1/2$ doublet $g_{\parallel}=2.43$ and $g_{\perp}=4.99$. The average $(g_{\parallel}+2g_{\perp})/3$ is 4.14. These values assume an effective $S'=1/2$; if referenced to the true $S=3/2$, $g_{\perp}=4.99/2=2.50$. Neglecting Zeeman matrix elements between this and the next higher doublet is justified as the axial zero-field splitting (ZFS) is very large, namely 165.4 cm^{-1} , corresponding to a D parameter of $165.4/2=82.7\text{ cm}^{-1}$. The dependence of the g values for the lowest Kramers' doublet on the axial splitting parameter δ is shown in Fig. 1, with all values referenced to $S'=1/2$. While $g_{zz}=g_{\parallel}$ is smaller than $g_{xx}=g_{\perp}$ for negative δ , corresponding to an axial elongation, the reverse obtains for positive δ , corresponding to an axial compression. The isotropic g value for zero δ is large, namely 4.29. Aasa and Vännngård¹⁰ have given an approximate expression for field-swept EPR signal intensity of $S=1/2$ systems in

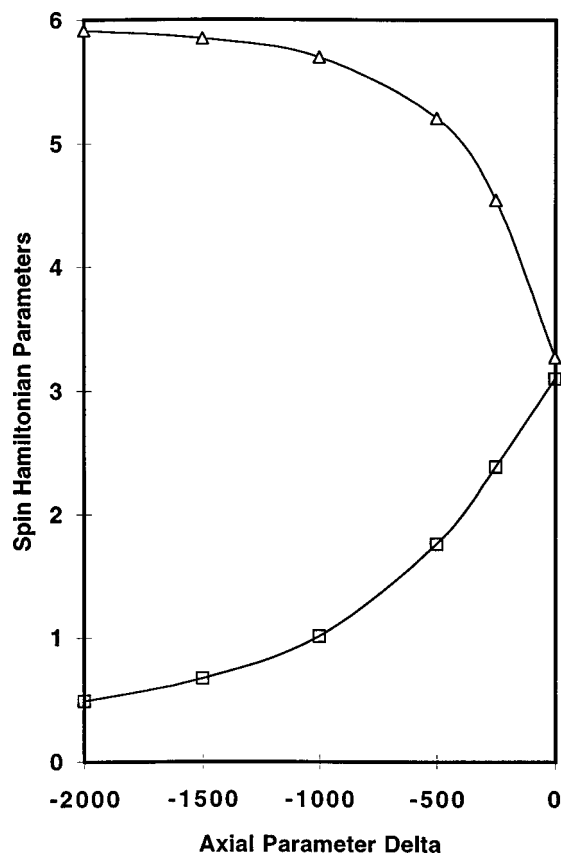


FIG. 2. Dependence of $g_{zz}=g_{||}$ (Δ) values for the upper Kramers' doublet ($g_{\perp}=0$ for this doublet) of high-spin Co(II) and of the zero-field splitting 2D (\square) between the upper and lower doublets in units of 10^2 cm^{-1} on the axial splitting parameter δ in cm^{-1} , with the g value referenced to $S'=1/2$. Values computed using $\gamma=1.424$ ($\Delta=9300 \text{ cm}^{-1}$) and $\zeta=435 \text{ cm}^{-1}$.

powders or frozen solutions in the presence of large g anisotropy. Their expression, which corresponds to $2/3$ times the root-mean-square of the principal values of the g tensor plus $1/3$ times their arithmetic mean, yields an intensity factor of 4.25 for the parameters given above.

In Fig. 2 we show the dependence of the ZFS splitting 2D in units of 10^2 cm^{-1} on the axial splitting parameter δ as calculated using $\gamma=-1.424$ and $\zeta=435 \text{ cm}^{-1}$. We note that the splitting increases as δ approaches 0, rising from 101 cm^{-1} for $\delta=-1000 \text{ cm}^{-1}$ to 310 cm^{-1} for $\delta=0$, where the splitting corresponds to a first-order spin-orbit splitting. We also show in Fig. 2 the dependence of $g_{zz}=g_{||}$ values for the upper Kramers' doublet with $|M_J|=3/2$ on δ ($g_{\perp}=0$ for this doublet), again assuming an effective $S'=1/2$). For example, with $\delta=-550 \text{ cm}^{-1}$, $g_{||}=5.29$, or if referenced to the true $S=3/2$, $g_{||}=5.29/3=1.76$.

This upper doublet is important in describing properties such as the magnetic susceptibility, as the 12-state electronic partition function at 298 K is 3.088, corresponding to which the Boltzmann population of each of the lowest energy doublet states is 0.324 and that of each of the next higher energy doublet states is almost half as much, namely 0.146. This partition function is fairly insensitive to δ , varying (for 298 K) from 3.072 for $\delta=-500 \text{ cm}^{-1}$ to 3.266 for $\delta=-1000 \text{ cm}^{-1}$, reflecting that most of the contribution is from

the lowest two doublets whose separation is decreasing from 176 to 101 cm^{-1} over this range of δ . The partition function may in fact be approximated by considering only the lowest two doublets (four states), giving a value of 2.900 at $T=298 \text{ K}$ for $\delta=-550 \text{ cm}^{-1}$ as compared to the 12-state value of 3.088.

ORTHORHOMBIC CRYSTAL FIELDS

We continue this analysis of the electronic structure and magnetic properties of approximately octahedral Co(II) complexes by considering the effects of an orthorhombic distortion superposed on a tetragonal distortion. In this section we take the axial (tetragonal) splitting parameter δ in Eq. (5) to have a value of -550 cm^{-1} , the value used³ by Figgis *et al.* in their fit of the magnetic susceptibility of the Co(II)(acac)₂(H₂O)₂ complex. They, however, did not consider orthorhombic fields in their study, as the susceptibility is essentially insensitive to small crystal-field splittings. As all six Kramers' doublets arising from a $^4T_{1g}$ multiplet transform as the $E'_g(\Gamma_{5g})$ irreducible representation of the spinor double-group D_{2h}^* it is necessary to set up and diagonalize the matrix of $H_{so}+H_{ax}+H_{ortho}$ in the 12-component $|M_S M_L\rangle$ basis. The effect of an orthorhombic field on a $^4T_{1g}$ multiplet may be expressed by the effective Hamiltonian H_{ortho} , where

$$H_{ortho} = \epsilon(L_x^2 - L_y^2). \quad (6)$$

An alternate form, appropriate for bond-bending deformations in the xy plane, is

$$H_{ortho} = \epsilon(L_x L_y + L_y L_x). \quad (7)$$

Using the 12-component basis $|M_S M_L\rangle$, the 12×12 matrix of H_{ortho} is diagonal in M_S but off-diagonal in M_L , with nonzero elements connecting $M_L=+1$ with $M_L=-1$; all nonzero elements of operator Eq. (6) equal ϵ (in units of \hbar^2), while those of Eq. (7) are $i\epsilon$ if the ket contains $M_L=+1$ and $-i\epsilon$ if the ket contains $M_L=-1$. As the interplay of the spin-orbit coupling and the tetragonal crystal field lift all degeneracies within a $^4T_{1g}$ multiplet save the Kramers' degeneracy, introduction of an orthorhombic field produces no additional splittings despite the resulting separation between the otherwise degenerate xz and yz pair of t_{2g} orbitals. As shown below, the effects of an orthorhombic crystal field are quite subtle but nevertheless important to consider.

Electronic magnetic moments, to which g values are proportional, are calculated as before, by assuming that all Zeeman energies are small compared to the zero-field splittings between Kramers' doublets produced by the interplay of the spin-orbit coupling and the low-symmetry crystal fields. That is, again we consider Zeeman interactions within each Kramers' pair but ignore interactions between pairs.

Again taking $\gamma=-1.424$ ($\Delta=9300 \text{ cm}^{-1}$), $\zeta=435 \text{ cm}^{-1}$, and $\delta=-550 \text{ cm}^{-1}$, together with $\epsilon=100 \text{ cm}^{-1}$, we obtain for the $|M_J|=1/2$ doublet $g_{zz}=2.40$, $g_{xx}=4.26$, and $g_{yy}=5.71$. The average $(g_{xx}+g_{yy}+g_{zz})/3$ is 4.12. These values assume an effective $S'=1/2$; if referenced to the true $S=3/2$, $g_{xx}=4.26/2=2.13$, and $g_{yy}=5.71/2=2.86$. For the $|M_J|=3/2$ doublet $g_{zz}=5.21$, $g_{xx}=-0.61$, and $g_{yy}=0.67$. The sign alternation between

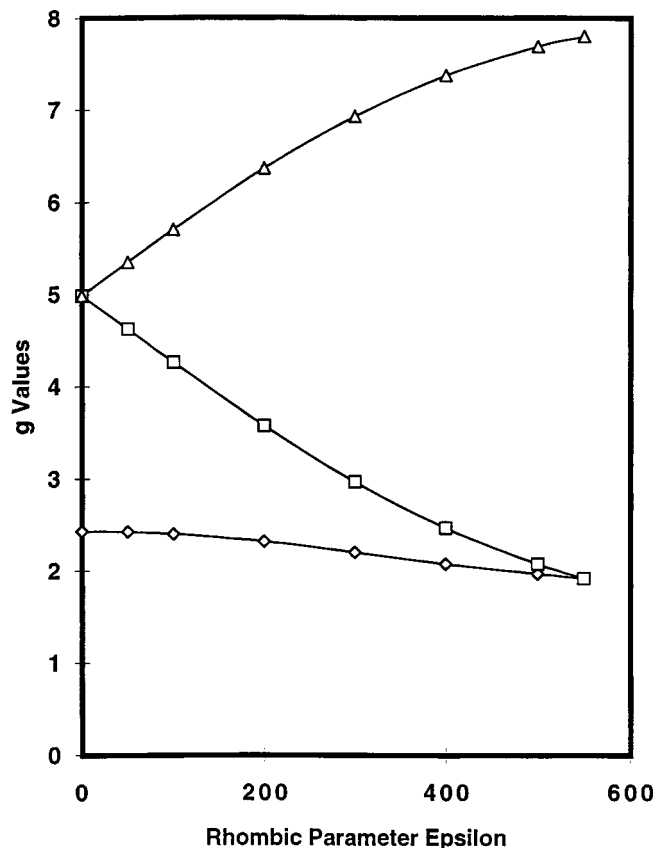


FIG. 3. Dependence of g_{xx} (□), g_{yy} (△), and g_{zz} (◇) values for the lowest Kramers' doublet of high-spin Co(II) on the orthorhombic splitting parameter ϵ in cm^{-1} , with all values referenced to $S' = 1/2$ and computed using $\gamma = 1.424$, $\zeta = 435 \text{ cm}^{-1}$, and an axial parameter δ of -550 cm^{-1} . For $\epsilon = 0$ the system is tetragonally elongated with respect to the z axis, while for $\epsilon = -\delta = 550 \text{ cm}^{-1}$ it is tetragonally compressed with respect to the y axis.

g_{xx} and g_{yy} means that the state which increases in energy with increasing induction B_x decreases with increasing B_y , but vice versa for its Kramers' partner. These values again assume an effective $S' = 1/2$; if referenced to the true $S = 3/2$, $g_{zz} = 5.21/3 = 1.74$. We do not reference the g_{xx} and g_{yy} values to $S' = 3/2$ since all matrix elements of S_x and S_y vanish within a pure 2-state spin manifold $|3/2 M_S\rangle = \pm 3/2$. The overall splitting between the two lowest doublets is 168.1 cm^{-1} , virtually unchanged from the value of 165.4 cm^{-1} for $\epsilon = 0$, while the 12-state partition function is 3.086 vs 3.088 for $\epsilon = 0$. Finally, the intensity factor calculated for $\epsilon = 100 \text{ cm}^{-1}$ using the Aasa and Vännegård¹⁰ expression is 4.27, insignificantly larger than the 4.25 value calculated assuming $\epsilon = 0$.

The dependencies of the g values for the lowest Kramers' doublets on the orthorhombic splitting parameter ϵ are shown in Fig. 3, with all values referenced to $S' = 1/2$. The axial parameter δ is taken as -550 cm^{-1} for this figure. The range of ϵ is taken from 0 to 550 cm^{-1} , at which value ($\epsilon/\delta = -1$) the system is in effect tetragonal but with an axial compression along the y -axis. (The g_{zz} and g_{xx} values in Fig. 3 merge for $\epsilon = 550 \text{ cm}^{-1}$ to form a new g_{\perp} .)

We have made several unsuccessful attempts to obtain the ESR spectrum of the $\text{Co(II)(acac)}_2(\text{H}_2\text{O})_2$ complex in frozen acetone (X -band), frozen chloroform (P -band), and pow-

dered solid (P -band) samples at temperatures as low as 4.2 K. All spectra were too broad and featureless to yield reliable g values. We do note in Fig. 1 the sensitivity of g_{zz} to δ in the neighborhood of $\delta = -500 \text{ cm}^{-1}$ and in Fig. 3 that of g_{xx} and g_{yy} to ϵ , suggesting "g-strain" as a major contributing factor to the breadth of the ESR signals.

In conclusion, the main consequences of rhombicity in the xy plane are first, to create a measurable anisotropy between the g_{xx} and g_{yy} values for the lowest Kramers' doublet and second, to make the g_{xx} and g_{yy} values for the upper doublet different from zero. The very large ZFS of the orbitally nondegenerate ${}^4A_{2g}$ component of the ${}^4T_{1g}$ multiplet of a distorted high-spin octahedral Co(II) complex precludes the use of a common g tensor to describe the magnetic moments and Zeeman energies of both the $|M_S| = 1/2$ and $|M_S| = 3/2$ Kramers' doublets arising from ${}^4A_{2g}$. While the entire 2×2 matrices of μ_x and μ_y vanish in the tetragonal case for the two Kramers' doublets with $M_J = \pm 3/2$ and the single doublet with $M_J = \pm 5/2$, so that $g_x = g_y = 0$ for these cases, the presence of an orthorhombic crystal field, as represented by the effective orbital angular momentum operator (6) or (7), mixes the basis function $|\pm 1/2, \pm 1\rangle$ in the $M_J = \pm 3/2$ axial eigenstates with the $M_J = \mp 1/2$ basis functions $|\pm 1/2, \mp 1\rangle$, and thus indirectly with other the $M_J = \mp 1/2$ basis functions $|\mp 1/2, 0\rangle$ and $|\mp 3/2, \pm 1\rangle$, as well as with the $M_J = \mp 5/2$ basis functions $|\mp 3/2, \mp 1\rangle$. (No orthorhombic mixings arise from the $|\pm 3/2, 0\rangle$ component of the $M_J = \pm 3/2$ axial eigenfunctions.) Because of these small mixings, each nominally $M_J = +3/2$ eigenstate is connected to its $M_J = -3/2$ Kramers' partner by the μ_x and μ_y operators so as to make g_{xx} and g_{yy} nonzero. Similarly, the $M_J = \pm 5/2$ axial eigenstates, identical to the basis functions $|\pm 3/2, \pm 1\rangle$, acquire via the rhombicity $|\pm 3/2, \mp 1\rangle$ character and hence acquire via the spin-orbit coupling $M_J = \pm 1/2$ character from the basis functions $|\pm 1/2, 0\rangle$ and $|\mp 1/2, \pm 1\rangle$, and less directly $M_J = \mp 3/2$ character from the basis functions $|\mp 3/2, 0\rangle$ and $|\mp 1/2, \mp 1\rangle$. These mixings make g_{xx} and g_{yy} nonzero for the Kramers' doublet derived from the $M_J = \pm 5/2$ axial eigenstates. Thus the interplay of the spin-orbit coupling and the axial and orthorhombic crystal fields makes all 12 eigenstates of a ${}^4T_{1g}$ manifold for a high-spin nearly octahedral Co(II) complex have nonzero magnetic moments and hence nonzero g values for arbitrary orientations of an external magnetic field with respect to the molecular axes. All six Kramers' doublets are qualitatively identical as they transform as the same (E'_g) irreducible representation of the spinor double-group D_{2h}^* , although they differ quantitatively in energy and g values.

MAGNETIC MOMENTS IN LOW-SYMMETRY CRYSTAL FIELDS

In the section on Octahedral Crystal Fields we gave the calculated effective magnetic moment μ_{eff} for our Co(II) complex as 5.14 B.M. at 298 K. This value was obtained using Griffith's expressions for an octahedral complex, thus invoking Van Vleck's theorem that low-symmetry crystal fields may be neglected. This assumption should be valid if the low-symmetry splittings are small, or at least not larger than kT , which equals 207 cm^{-1} at 298 K. As the axial

splitting parameter δ is most likely larger than this in magnitude, we now describe our calculation of μ_{eff} for high-spin Co(II) complexes with arbitrary tetragonal and orthorhombic crystal fields.

The procedure is essentially a generalization of that given by Eqs. (4a)–(4d), namely,

$$\mu_{\text{eff}}^2(T) = \sum W_i \mu_{\text{eff}}^2(i) / \sum W_i, \quad (8)$$

where the W_i are Boltzmann factors for the i th Kramers' doublet. Each contribution contains two types of terms; the first are the temperature-independent (aside from Boltzmann factors) "diagonal" contributions $\mu_x^2 + \mu_y^2 + \mu_z^2$ based on the expectation values of the components of $\mu = \beta(\gamma\mathbf{L} + g_e\mathbf{S})$ with respect to each doublet, while the second are temperature-dependent (in addition to Boltzmann factors) "off-diagonal" contributions based on matrix elements of the components of μ between a given doublet and each of the other five doublets. The latter contributions are of the type associated with the so-called temperature independent magnetic susceptibility, as the relationship [Eq. (4a)] between X and μ_{eff}^2 involves division by T , that is,

$$X(T) = \mu_0 N_0 \beta^2 \mu_{\text{eff}}^2(T) / 3kT. \quad (9)$$

In the spin-only case μ_{eff}^2 has the well-known value $g_e^2 S(S+1)$, which is 15.0345 for $S=3/2$.

Implementation of the procedure from this point is much like the calculation of g values described in the Orthorhombic Crystal Fields section; the 12×12 matrices of each component of μ are transformed to the basis of the eigenstates of $H_{\text{so}} + H_{\text{ax}} + H_{\text{ortho}}$ from their original $|M_S M_L\rangle$ basis. The diagonal contributions described above are proportional to spatially averaged g values, while the off-diagonal contributions, each containing a factor of kT divided by the energy difference between the perturbing state and the reference state, represent the interactions not included in the g -value calculations. That is, there is a sum over six Kramers' doublets, each having not only a Boltzmann population and diagonal contributions, but also a sum of off-diagonal contributions over the other five doublets.

In Fig. 4 we show a comparison of the temperature dependence on the range 78–295 K of our μ_{eff} values calculated using $\gamma = -1.424$ and $\zeta = 435 \text{ cm}^{-1}$, together with an orthorhombic parameter ϵ of zero, with the experimental temperature dependence reported in Ref. 3 for Co(II)(acac)₂(H₂O)₂. The four calculated curves are for values of -250 , -550 , -650 , and -850 cm^{-1} for the orbital splitting parameter δ . As δ becomes more negative, the 12-state electronic partition function q rises slightly and μ_{eff} , which contains a factor of $q^{-1/2}$, falls. Our μ_{eff} values are fairly insensitive to small variations in δ , with the best agreement for a δ value of -550 to -650 cm^{-1} . Figgis *et al.* fit their measurements³ to a model with a splitting parameter of 550 cm^{-1} (opposite sign convention to our δ), pointing out that their data can also be fitted using an oppositely-signed parameter of -1040 cm^{-1} , corresponding to $\delta = +1040 \text{ cm}^{-1}$, implying that 4E_g lies below ${}^4A_{2g}$. The latter interpretation may be rejected based on the structure of Co(II)(acac)₂(H₂O)₂, with longer bonds to water oxygens than to acac oxygens. Introduction of an orthorhombic split-

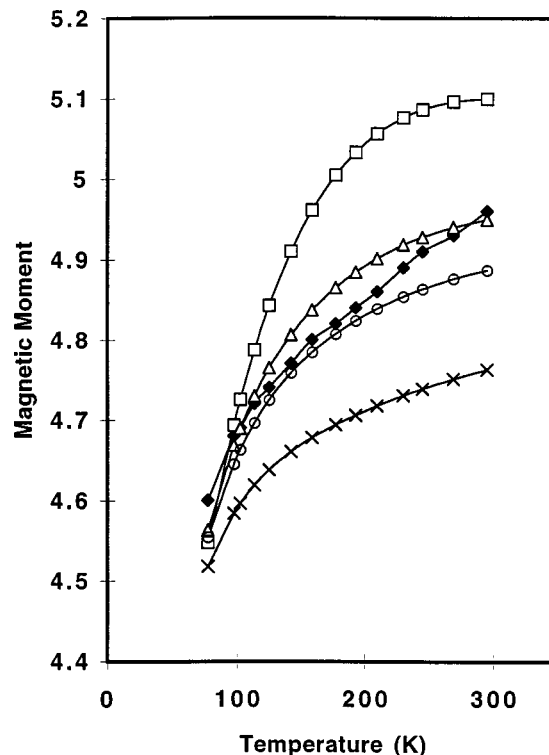


FIG. 4. Comparison of calculated magnetic moment in Bohr magnetons for tetragonal high-spin Co(II) vs temperature in K with experimental values from Ref. 3 for Co(acac)₂(H₂O)₂. The experimental values lie on the curve with points marked \blacklozenge , while the curves with points marked \square , \triangle , \circ , and \times are for values of the tetragonal orbital splitting parameter δ of -250 , -550 , -650 , and -850 cm^{-1} , respectively.

ting parameter $\epsilon = 100 \text{ cm}^{-1}$ leaves the μ_{eff} value for $\delta = -550 \text{ cm}^{-1}$ virtually unchanged from the 4.95 B.M. value obtained with $\epsilon = 0$, and is insignificantly larger, namely 4.96 B.M., for a much larger $\epsilon = 400 \text{ cm}^{-1}$, thus validating the neglect of such small orthorhombic terms in accord with Van Vleck's theorem. The tetragonal field does, however, lower the calculated moment about 4% from its value for an octahedral complex.

SUSCEPTIBILITY ANISOTROPIES AND PROTON PSEUDOCONTACT SHIFTS

In the previous section we outlined our procedure for calculation of the (dimensionless) effective Bohr magneton number μ_{eff} for high-spin Co(III) complexes. Although the values given there correspond to spatial averages, it is straight forward to calculate instead values corresponding to principal values X_{ii} (in $\text{m}^3 \text{ mol}^{-1}$) of the molar susceptibility tensor by simply selecting the magnetic moment operator $\mu = \beta(\gamma\mathbf{L} + g_e\mathbf{S})$ to lie along the desired principal direction. These values may then be used to calculate the isotropic pseudocontact shift^{11,12} contribution δ^{pc} . For a proton at a distance R from the paramagnetic center and with direction cosines $\cos \theta_x$, $\cos \theta_y$, and $\cos \theta_z$ with respect to the principal axes x , y , and z of the complex, δ^{pc} , an example of a " $\delta\delta$," may be written as

$$\delta^{pc} = -(\Delta B/B_0) = (2/3N_0R^3) \sum_i X_{ii} P_2(\cos \theta_i), \quad (10)$$

where B_0 denotes the field strength (or induction) at which resonance would occur for a diamagnetic counterpart of the paramagnetic complex, $\Delta B = B - B_0$ is the difference between B for the paramagnetic complex and B_0 at fixed rf frequency, the summation is over the principal directions x , y , and z of the susceptibility tensor, and $P_2(\cos \theta_i) = (3 \cos^2 \theta_i - 1)/2$. Equation (10) is a variation of Kurland and McGarvey's equation¹¹ which was expressed in terms of the pair of proton angular coordinates Ω and ψ ; we prefer the symmetric form of Eq. (10). Our sign convention in Eq. (10) follows current NMR usage¹³ and thus is opposite to that of Kurland and McGarvey. That is, since a "down-field" shift from TMS is assigned a positive δ value, a positive δ^{pc} (or " $\delta\delta$ ") contribution results in a greater "down-field" total shift, while a negative δ^{pc} contribution results in a smaller "down-field" total shift.

Introducing into Eq. (10) the constraint

$$\sum_i P_2(\cos \theta_i) = 0 \quad (11)$$

leads to an alternative form

$$\begin{aligned} \delta^{pc} = & -(2/3N_0R^3)[(X_{zz} - X_{xx})P_2(\cos \theta_x) \\ & + (X_{zz} - X_{yy})P_2(\cos \theta_y)]. \end{aligned} \quad (12)$$

Equation (12) displays clearly the well-known result that δ^{pc} vanishes if X is isotropic and that it reduces to

$$\delta^{pc} = (2/3N_0R^3)[(X_{\parallel} - X_{\perp})P_2(\cos \theta_z)] \quad (13)$$

if X is axially symmetric with respect to the z axis. The sign conventions implied by Eq. (13) are such that δ^{pc} is positive (a "down-field" shift contribution) for a proton lying on the z -axis ($P_2(\cos \theta_z) = 1$) if the susceptibility anisotropy ($X_{\parallel} - X_{\perp}$) is positive.

In Fig. 5 we show the dependence of the principal values of the magnetic susceptibility tensor X/N_0 in units of $\text{\AA}^3 \text{ molecule}^{-1}$ for high-spin Co(II) at 298 K on the axial (tetragonal) splitting parameter δ in cm^{-1} , as computed using $\gamma = 1.424$ and $\zeta = 435 \text{ cm}^{-1}$. The points denoted by the symbols \diamond and \square correspond to X_{\perp} and X_{\parallel} , respectively, each divided by N_0 , while those denoted by Δ correspond to the weighted X_{ave} . For negative values of the axial parameter δ the susceptibility X_{\perp} is greater than X_{\parallel} , so that δ^{pc} is negative for a proton lying on, or nearly on, the z axis. We note the close resemblance in the shape of the plot of X_{\parallel} in Fig. 5 to that of g_{\parallel} in Fig. 1, each vs the axial parameter δ , and similarly of the plot of the X_{\perp} in Fig. 5 to that of g_{\perp} in Fig. 1. If only the lowest Kramers' doublet were thermally occupied, the X values at a given temperature would scale as the squares of the corresponding g values. Our X values at 298 K are somewhat less sensitive to δ than the corresponding squares of g values as the second lowest Kramers' doublet has significant thermal population; with an electronic partition function q at 298 K of approximately 3, two-thirds of the complexes are in the lowest Kramers' doublet, with one-third in the next lowest.

The complex $\text{Co(II)(acac)}_2(\text{H}_2\text{O})_2$ has four water protons at an angle θ_z of 14° and a distance of 2.90 \AA from the Co(II) ion, two methine protons in the equatorial plane ($\theta_z = 90^\circ$) at a distance of 4.35 \AA , and twelve methyl protons at

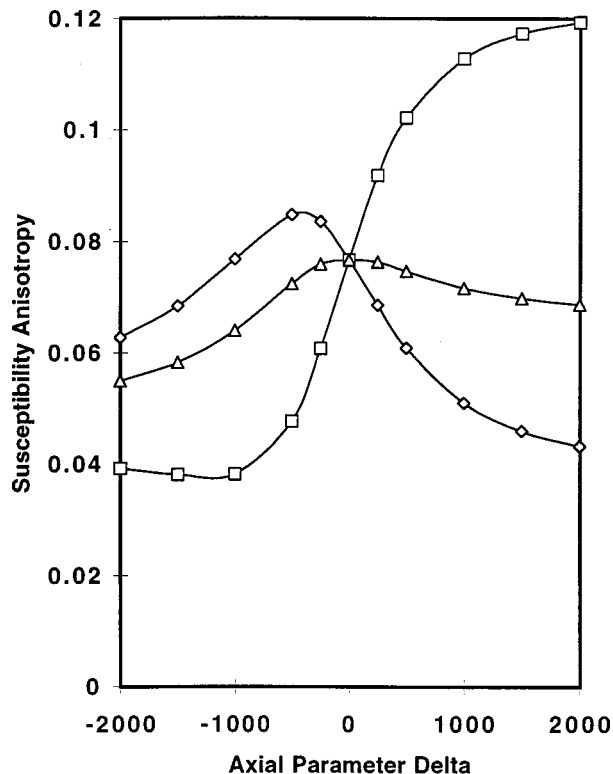


FIG. 5. Dependence of the principal values of the magnetic susceptibility tensor X/N_0 in units of $\text{\AA}^3 \text{ molecule}^{-1}$ for high-spin Co(II) at 298 K on the axial (tetragonal) splitting parameter δ in cm^{-1} , as computed using $\gamma = 1.424$ and $\zeta = 435 \text{ cm}^{-1}$. The points denoted by the symbols \diamond and \square correspond to X_{\perp} and X_{\parallel} , respectively, each divided by N_0 , while those denoted by Δ correspond to the weighted X_{ave} .

a distance of 4.76 \AA . Assuming axial (D_{4h}) symmetry as an approximation, application of Eq. (13) with an assumed value of $\delta = -550 \text{ cm}^{-1}$, for which $X_{\parallel} = 0.0458$ and $X_{\perp} = 0.0844 \text{ \AA}^3 \text{ molecule}^{-1}$, leads to δ^{pc} values of -961 ppm for the water protons, $+155$ ppm for the methine protons, and $+119$ ppm for the methyl protons, these assumed to lie in the equatorial plane ($\theta_z \approx 90^\circ$). With a smaller tetragonal field corresponding to $\delta = -250 \text{ cm}^{-1}$, $X_{\parallel} = 0.0607$, and $X_{\perp} = 0.0835 \text{ \AA}^3 \text{ molecule}^{-1}$, leading to δ^{pc} values of -569 , $+92$, and $+70$ ppm for the water, methine, and methyl protons, respectively. With either value of the axial parameter δ there is a somewhat smaller pseudocontact shift from the methyl protons than for the methine protons, a conclusion consistent with the larger distance of the methyl protons from the Co(II) center. The susceptibility anisotropy $|\Delta X|/X_{\text{av}}$ is about 54% and 30% for these δ values, larger than the approximate crystal anisotropy of 14% at 300 K as reported¹⁴ by Brown *et al.* However the two complexes related by a glide plane in the monoclinic ($P2_1/c$) crystal have their Co-OH₂ axes almost perpendicular, greatly reducing the crystal magnetic anisotropy. Finally we have also computed the susceptibility anisotropies $X_{zz} - X_{xx}$ and $X_{zz} - X_{yy}$ as a function of the orthorhombic parameter ϵ for fixed δ values, but have not displayed these results.

AB INITIO CALCULATIONS

In order to explore in more detail the relationship between the molecular structure of the *bis-acac* Co(II) complex

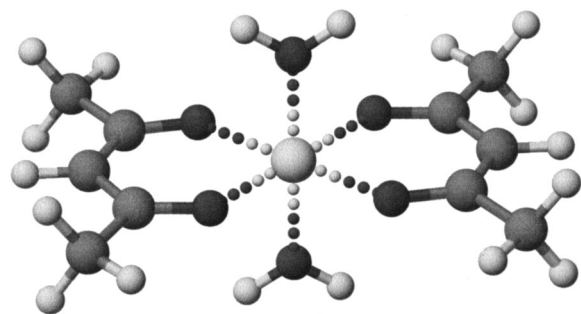


FIG. 6. Structure of $\text{Zn}(\text{acac})_2(\text{H}_2\text{O})_2$ complex with D_{2h} symmetry as optimized at the HF/3-21G level using analytic gradients and as used in calculations at various levels for the complexes $\text{M}(\text{acac})_2(\text{H}_2\text{O})_2$, $\text{M}=\text{Mn}$, Co , and Ni . The optimized Zn–O separations were found to be 2.026 Å for the acac O atoms and 2.060 Å for the water O atoms.

and its electronic properties including the “crystal-field” splittings and electron spin densities, we have carried out a number of *ab initio* calculations with the GAUSSIAN 94 program.¹⁵ We first optimized the geometry of the closed-shell $\text{Zn}(\text{acac})_2(\text{H}_2\text{O})_2$ complex at the SCF (HF) level by using analytic gradients and the split-valence basis set 3-21G. This computational level is designated as HF/3-21G. All structural parameters were optimized subject to the constraint of D_{2h} symmetry imposed by having the water ligands oriented with their H–H directions parallel to the axis connecting the methine carbons, and by having the methyl groups oriented with one H atom of each lying in the molecular plane and pointing “out” (Fig. 6). The optimized Zn–O separations were found to be 2.026 Å for the acac O atoms and 2.060 Å for the water O atoms. While the former is close to the value of 2.042 Å found in the x-ray structure of the Co(II) complex, the latter is clearly shorter than the observed 2.215 Å value for the distance to the water O atoms. Nevertheless we have used the HF/3-21G optimized structure of $\text{Zn}(\text{acac})_2(\text{H}_2\text{O})_2$ as a reasonable estimate of the structure of other $\text{M}(\text{acac})_2(\text{H}_2\text{O})_2$ complexes.

We next considered the high-spin Mn(II) complex $\text{Mn}(\text{acac})_2(\text{H}_2\text{O})_2$. The ground multiplet is 6A_g in D_{2h} symmetry, with single occupancy of each of the mostly Mn(3*d*) MOs, thus avoiding the complication found in the corresponding Ni(II) and Co(II) complexes of having both singly and doubly occupied mostly M(3*d*) MOs. Calculations were first made at the unrestricted Hartree–Fock (UHF) level both with the 3-21G basis set and with a general basis set¹⁶ of double-zeta quality for each orbital type, augmented by a diffuse *d*-function with exponent 0.0154, so that the basis is

triple-zeta for Mn(3*d*). These computations are designated as UHF/3-21G and UHF/GEN, respectively. Specifically the general basis set is of the form 31 for H atoms, 6111/41 for C and O atoms, and 62111111/331211/321 for the Mn atom. Calculations were also made at the restricted open-shell Hartree–Fock (ROHF) level with both of the above basis sets. These computations are designated as ROHF/3-21G and ROHF/GEN, respectively. In Table I we present the total energies, Mulliken charges on Mn, and the energies of the mostly Mn(3*d*) MOs for each of the four computations on the Mn(II) complex. While the UHF and ROHF values of the Mulliken charges on Mn all lie in the range 1.1–1.3, the UHF orbital energies are very much larger than their ROHF counterparts. An octahedral splitting parameter Δ may be obtained by subtracting the average of the energies of the three lowest (t_{2g}) MOs from that of the two highest (e_g) MOs; this parameter is found to be quite large, namely, about 20 210 and 19 915 cm^{-1} at the UHF/3-21G and UHF/GEN levels, respectively, but only 5580 and 7130 cm^{-1} at the ROHF/3-21G and ROHF/GEN levels, respectively. A reasonable value of D for this complex would probably be around 12 000 cm^{-1} , roughly the mean of the UHF and ROHF values.

In Table II we show spin results for the high-spin $\text{Mn}(\text{acac})_2(\text{H}_2\text{O})_2$ complex. As is well-known, the ROHF wave functions are eigenfunctions of S^2 and S_z , while the UHF functions are eigenfunctions of S_z only, so that ROHF spin densities for a state with $M_S > 0$ cannot be negative. The calculated UHF/GEN ($M_S = +5/2$) spin densities for the methine and methyl protons are quite small but opposite in sign, namely, -1.5×10^{-5} and 7.2×10^{-5} , respectively; the value for the water protons is much higher, namely, 4.3×10^{-3} . (The methyl value is a weighted average of the spin densities for in-plane and out-of-plane protons in D_{2h} symmetry.) Also tabulated are Fermi contact values in Bohr⁻³ for the three types of proton sites. These values represent the single-particle density at the respective nuclei and are roughly proportional to the corresponding spin densities, the latter obtained from the difference of Mulliken population analyses for alpha and beta spin electrons. We note that while the spin densities for methine and methyl protons have opposite signs, the Fermi contact values are both positive. These values could be used to calculate electron–nuclear spin–spin coupling constants and Fermi contact proton nmr shifts. Indeed we have used Fermi contact values for the corresponding Co(II) complex to calculate contact shifts. However our conclusion is that the values, except for the water proton

TABLE I. *Ab initio* energy and charge results for $\text{Mn}(\text{acac})_2(\text{OH}_2)_2$.

| Level | E^a | $Q(\text{Mn})^b$ | $\epsilon(b_{2g})^c$ | $\epsilon(b_{3g})$ | $\epsilon(a_g)$ | $\epsilon(a_g)$ | $\epsilon(b_{1g})$ |
|------------|---------------|------------------|----------------------|--------------------|-----------------|-----------------|--------------------|
| UHF/3-12G | −1 978.146 64 | 1.118 | 0 | 3909 | 5954 | 19 248 | 27 750 |
| UHF/GEN | −1 988.062 15 | 1.313 | 0 | 4297 | 6163 | 18 109 | 28 694 |
| ROHF/3-21G | −1 978.145 71 | 1.118 | 0 | 239 | 481 | 5 116 | 6 516 |
| ROHF/GEN | −1 988.060 34 | 1.317 | 0 | 281 | 709 | 6 701 | 8 224 |

^aEnergy in hartrees for the 6A_g multiplet. Geometry optimized at the HF/3-21G level for the Zn(II) complex.

^bMulliken charge for Mn.

^cOrbital energies of mostly Mn(3*d*) MO's in cm^{-1} relative to that of lowest (b_{2g}) mostly Mn(3*d*) MO.

TABLE II. *Ab initio* spin results for Mn(acaca)₂(OH₂)₂.

| Level | $\langle S^2 \rangle^a$ | $\rho_s(\text{Mn})^b$ | $\rho_s(\text{CH})^c$ | $\rho_s(\text{CH}_3)$ | $\rho_s(\text{H}_2\text{O})$ | $F(\text{CH})^d$ | $F(\text{CH}_3)$ | $F(\text{H}_2\text{O})$ |
|------------|-------------------------|-----------------------|-----------------------|-----------------------|------------------------------|----------------------|----------------------|-------------------------|
| UHF/3-12G | 8.751 | 4.934 | 1.6×10^{-4} | 1.4×10^{-4} | 5.2×10^{-3} | 5.0×10^{-6} | 4.2×10^{-5} | 1.5×10^{-3} |
| UHF/GEN | 8.752 | 4.968 | -1.5×10^{-5} | 7.2×10^{-5} | 4.3×10^{-3} | 2.0×10^{-6} | 3.2×10^{-5} | 1.4×10^{-3} |
| ROHF/3-21G | 8.750 | 4.905 | 1.2×10^{-4} | 9.4×10^{-5} | 2.8×10^{-3} | 3.1×10^{-5} | 2.9×10^{-5} | 9.0×10^{-4} |
| ROHF/GEN | 8.750 | 4.928 | 8.6×10^{-5} | 1.0×10^{-4} | 1.8×10^{-3} | 3.8×10^{-5} | 3.0×10^{-5} | 7.6×10^{-4} |

^aMean value of S^2 in units of \hbar^2 .

^bSpin densities at Mn site.

^cSpin densities at designated proton sites; values for methyl protons are averaged.

^dFermi contact in Bohr³ at designated proton sites; values for methyl protons are averaged.

values, are too small to be computationally significant.

We next carried out calculations at the UHF/3-21G level for the Ni(II) and Co(II) M(acac)₂(H₂O)₂ complexes, each taken to have the HF/3-21G optimized geometry of the corresponding Zn(II) complex. For the Ni complex the ground multiplet is expected to be ³B_{1g} in D_{2h} symmetry [unpaired electrons in mostly Ni(3d)*a_g* and *b_{1g}* MOs], corresponding to ³A_{2g} in O_h symmetry. Indeed we find ³B_{1g} and ³B_{3g} multiplets to have UHF/3-21G energies of -2 333.359 93 and -2 333.325 70 hartrees, respectively. The latter multiplet, lying 7513 cm⁻¹ higher in energy than the ³B_{1g} multiplet, has unpaired electrons in mostly Ni(3d)*b_{2g}* and *b_{1g}* MOs, thus corresponding to one component of the octahedral ³T_{1g} and ³T_{2g} multiplets (mixed in D_{2h}) arising from the configuration *t_{2g}⁵e_g³*. Thus we have found two of the ten spin triplets arising from the *d⁸* configuration (³A_g + ³B_{1g} + ³B_{2g} + ³B_{3g} in D_{2h} symmetry), including the expected lowest energy ³B_{1g} multiplet arising the octahedral configuration *t_{2g}⁶e_g²*.

For the Co complex the ground multiplet is expected to be ⁴B_{1g} in D_{2h} symmetry [unpaired electrons in mostly Co(3d)*a_g*, *a_g*, and *b_{1g}* MOs], corresponding to one spatial component of ⁴T_{1g} in O_h symmetry. A total of ten spin quartets arise from the *d⁷* configuration (⁴A_g + ³B_{1g} + ³B_{2g} + ³B_{3g} in D_{2h} symmetry). We have found three of these multiplets at the UHF/3-21G level, namely ⁴B_{1g} and ⁴B_{2g}, both arising from the octahedral configuration *t_{2g}⁵e_g²*, as well as ⁴A_g, arising from *t_{2g}⁴e_g³*. In Table III we summarize their energies and other properties. A surprise is that the lowest energy of the three is that of the ⁴B_{2g} multiplet, with unpaired electrons in mostly Co(3d)*a_g*, *b_{1g}*, and *b_{3g}* MOs, thus differing from the expected lowest energy multiplet by a rearrangement within the *t_{2g}* subshell, namely, a promotion

of a β electron from a *b_{3g}* MO to an *a_g* MO. As shown in Table III, the energy difference between the ⁴B_{1g} and ⁴B_{2g} multiplets is nearly the same at the UHF and MP2 levels, namely, 3035 and 2763 cm⁻¹, respectively. A simple orbital energy interpretation of this energy ordering is that the *b_{3g}* MO, or *yz* with acac ligands in the *xy* plane and with methine groups on the $\pm x$ axes, is the highest in energy of the three *t_{2g}* MOs, a result which in conflict with the expectation of a crystal-field analysis based on the assumption that the tetragonal parameter δ [Eq. (5)] is negative and that the orthorhombic parameter ϵ [Eq. (6)] is smaller in magnitude than δ .

The relationship between one-electron orbital energies λ_i and the effective multiplet splitting parameter δ of Eq. (5) may be expressed in the strong-field description of Eq. (2) as

$$\delta = (3/4) \sin^2 \alpha (\lambda_\epsilon - \lambda_\theta) + (\sin^2 \alpha - \cos^2 \alpha) (\lambda_\zeta - \lambda_{\eta,\xi}). \quad (14)$$

The subscripts θ and ϵ denote the *e_g* orbitals ($3z^2 - r^2$ and *xy* in our coordinate system), while ξ , η , and ζ denote the *t_{2g}* orbitals (*yz*, *xz*, and $x^2 - y^2$). In the strong-field limit $\alpha \rightarrow 0$, corresponding to a pure *t_{2g}⁵(²T_{2g})e_g²(³A_{2g})⁴T_{1g}* multiplet, the only contribution to δ arises from the tetragonal splitting of the octahedral *t_{2g}* orbitals, that is, $\delta = -(\lambda_\zeta - \lambda_{\eta,\xi})$. (The *e_g²* subshell is half-filled and thus not affected in first order by a tetragonal field.) With $B = 980 \text{ cm}^{-1}$ and $\Delta = 9 300 \text{ cm}^{-1}$ as before, the ⁴T_{1g} multiplet is close to this limit, with $\sin^2 \alpha = 0.0806$ and $\cos^2 \alpha = 0.9194$, so that $\delta = 0.0604(\lambda_\epsilon - \lambda_\theta) - 0.8388(\lambda_\zeta - \lambda_{\eta,\xi})$. Using orbital energies for the Mn(II) complex from Table I as estimates of the λ_i , the orbital energy differences $(\lambda_\epsilon - \lambda_\theta) = (\lambda_{b_{1g}} - \lambda_{a_g})$ and $(\lambda_\zeta - \lambda_{\eta,\xi}) = (\lambda_{a_g} - \lambda_{b_{2g}, b_{3g}})$ are both positive. As the first difference has a positive coefficient but the second a negative coefficient, the two contributions to δ tend to cancel, leading to δ values of approximately -2800 cm⁻¹ using UHF values of the λ_i from Table I, but only approximately -250 cm⁻¹ using ROHF values. (The dependence on the basis set is comparatively slight.) While the UHF values are clearly much too large in magnitude, and the ROHF values too small, the dominate contribution for each is that arising from the positive orbital energy difference $(\lambda_\zeta - \lambda_{\eta,\xi})$ within the *t_{2g}* subset.

TABLE III. *Ab initio* energy, charge, and spin results for Co(acaca)₂(OH₂)₂.

| Multiplet | Level | E^a | ΔE^b | $Q(\text{Co})^c$ | $\langle S^2 \rangle^d$ |
|------------------------------|-----------|---------------|--------------|------------------|-------------------------|
| ⁴ B _{2g} | UHF/3-12G | -2 208.541 45 | 0 | 1.054 | 3.751 |
| | MP2/3-21G | -2 210.254 28 | 0 | 0.772 | 3.750 |
| ⁴ B _{1g} | UHF/3-21G | -2 208.527 62 | 3035 | 1.055 | 3.752 |
| | MP2/3-21G | -2 210.241 69 | 2763 | 0.776 | 3.751 |
| ⁴ A _g | UHF/3-21G | -2 208.521 47 | 4385 | 1.068 | 3.751 |
| | MP2/3-21G | -2 210.233 59 | 4540 | 0.788 | 3.750 |

^aEnergy in hartrees for designated multiplet. Geometry optimized at the HF/3-21G level for the Zn(II) complex.

^bEnergy difference in cm⁻¹ relative to the ⁴B_{2g} multiplet.

^cMulliken charge for Co.

^dMean value for S^2 in units of \hbar^2 .

NMR SPECTRA OF Co(acac)₂(H₂O)₂

We have obtained proton NMR chemical shifts using a Bruker AC 200 (200 MHz) spectrometer and a sample of

Co(acac)₂(H₂O)₂ synthesized by the method of Ellern and Ragsdale.¹⁷ The orange–red complex was characterized by its IR spectrum and room temperature magnetic susceptibility, both agreeing with literature.^{18,19} The samples contained 20 mM Co(acac)₂(H₂O)₂ in *d*₆-DMSO in a mixed solvent containing 1% v/v D₂O, 0.5% v/v toluene, and 0.03% v/v TMS. The chemical shifts were measured at 20 ± 1 °C with respect to the toluene methyl peak (2.37 ppm) which had previously been referenced to internal TMS. The water peak was assigned by sequential addition of water aliquots, but could not be assigned as arising from coordinated water. The methyl and methine peaks gave integrated areas in the expected 6:1 ratio.

Taking the parent acid as a reference, the methyl proton resonance in Co(acac)₂(H₂O)₂ occurs at a shift δ of +23.1 ppm, that is, down-field from methyl in Hacac, while the methine proton resonance occurs at a shift of +4.7 ppm, down-field from methine in Hacac. Referenced in this way, the difference of +18.4 ppm between the methyl and methine shifts in the Co(II) complex should represent the difference in the sum of the contact and pseudocontact contributions, δ^{con} and δ^{pc} , respectively, between the two proton types. Our δ^{pc} values as calculated from the anisotropy in the computed susceptibility yield a difference of –22 to –35 ppm between methyl and methine protons, with the less negative value associated with an axial splitting parameter δ of –250 cm^{–1} and the more negative with δ of –550 cm^{–1}. Agreement with the observed total isotropic shift difference would then require that the difference in the contact shifts δ^{con} be of the order of +40 ppm or greater. We have measured a difference of +20.3 ppm between the methyl and methine shifts in the related complex Ni(acac)₂(H₂O)₂, with each shift again taken relative to its counterpart in the parent acid Hacac. This difference presumably arises solely from δ^{con} contributions, as the Ni(II) ion has a largely spin-only magnetic moment. Replacing Ni(II) by high-spin Co(II) creates a hole in a *t*_{2g} MO, specifically *a*_g(*x*²–*y*²) in *D*_{2h} with acac oxygens lying between the *x* and *y* axes in the *xy* plane. This MO not only has density in the plane of the acac ligands but has lobes pointing in the directions of the methine protons. Indeed our *ab initio* calculations, while not accurate enough to yield reliable values of the very small spin densities at the proton positions, do indicate a significant (order of magnitude) increase in spin density at the methine protons in going from Ni(II) to Co(II), but only a modest change at the methyl protons. Thus we find it not unreasonable to suggest that the difference between the contact contributions to the shift for methyl and methine protons for the Co(II) complex is much larger than the +20.3 ppm difference we measure for the Ni(II) complex.

SUMMARY

We have analyzed the electronic structure of the high-spin 3*d*⁷ Co(II) ion in the approximately octahedral Co(II)(acac)₂(H₂O)₂ complex in terms of crystal fields of descending symmetry from octahedral to orthorhombic. The energies and wave functions resulting from the interplay of these fields with the spin–orbit coupling have been used to obtain zero-field splittings, magnetic moments, magnetic

susceptibilities, and *g* values for the complex. These results in turn have been used in an analysis of the pseudocontact proton NMR shifts (δ^{pc}) in the Co(II)(acac)₂(H₂O)₂ complex. While the results are sensitive to the selected crystal-field splitting parameters, we typically find very negative values of δ^{pc} for the water protons, namely –500 to –1000 ppm, while the values for the methine and methyl protons are positive and smaller in magnitude, typically +90 to +150 ppm for the methine protons and +70 to +120 ppm for the methyl protons. We have used these computed pseudocontact shifts in an analysis of our measured shifts for these two proton types in Co(II)(acac)₂(H₂O)₂.

We may summarize the crystal field analysis by outlining here a sequence of steps for making semiquantitative estimates of pseudocontact proton NMR shifts (δ^{pc}) in high-spin Co(II) complexes:

- Extract principal *g* values for the lowest Kramers' doublet from ESR spectra.
- Use these values in a crystal-field analysis such as ours to estimate principal *g* values for the upper (second) Kramers' doublet and the excitation energy 2*D* to this doublet. (Information about the upper doublet is needed as its Boltzmann population at 298 K is roughly one-half of that of the lower doublet.)
- Use *g* values from (a) and (b) together with the splitting 2*D* and the temperature *T* to calculate anisotropic thermally averaged magnetic moments and susceptibilities.
- Use the anisotropic susceptibilities to calculate the pseudocontact proton NMR shifts (δ^{pc}) by conventional expressions.¹¹

We have also explored the relationship between molecular structure and crystal-field splittings for this complex via a series of *ab initio* electronic structure calculations for the M(II)(acac)₂(H₂O)₂ complexes with M=Mn, Co, Ni, and Zn. Both UHF and ROHF calculations on the Mn(II) complex, in which each mostly-3*d* MO is singly occupied, yield qualitatively reasonable tetragonal and orthorhombic orbital splitting parameters. For the Ni complex the lowest energy multiplet found is, as expected, ³*B*_{1g} in *D*_{2h} symmetry, corresponding to ³*A*_{2g} in *O*_h symmetry. Finally we conclude that the Fermi contact densities calculated from UHF wave functions for the Mn, Co, and Ni complexes, are, except for the water proton values, too small to yield computationally significant Fermi contact proton NMR shifts.

¹R. Sharp, S. M. Abernathy, and L. L. Lohr, J. Chem. Phys. **107**, 7620 (1997).

²S. M. Abernathy, J. C. Miller, L. L. Lohr, and R. R. Sharp, J. Chem. Phys. **109**, 4035 (1998).

³B. N. Figgis, M. Gerloch, J. Lewis, F. E. Mabbs, and G. A. Webb, J. Chem. Soc. A **1968**, 2086.

⁴J. S. Griffith, *The Theory of Transition Metal Ions* (Cambridge University Press, Cambridge, 1961), pp. 235 and 411.

⁵J. S. Griffith, in Ref. 4, pp. 272–273.

⁶J. S. Griffith, in Ref. 4, pp. 265–269.

⁷S. M. Abernathy, Ph.D. dissertation, University of Michigan, Ann Arbor, MI, 1997, p. 116.

⁸G. J. Bullen, Acta Crystallogr. **12**, 703 (1959).

⁹J. S. Griffith, in Ref. 4, pp. 360–363.

- ¹⁰R. Aasa and T. Vännngård, *J. Magn. Reson.* **19**, 308 (1975).
- ¹¹R. J. Kurland and B. R. McGarvey, *J. Magn. Reson.* **2**, 286 (1970).
- ¹²(a) W. DeW. Horrocks, Jr., R. H. Fischer, and J. R. Hutchison, *J. Am. Chem. Soc.* **88**, 2436 (1966); (b) J. P. Jesson, *J. Chem. Phys.* **47**, 579 (1967); **47**, 582 (1967); (c) B. R. McGarvey and J. Pearlman, *J. Magn. Reson.* **1**, 178 (1969); (d) B. R. McGarvey, *Inorg. Chem.* **34**, 6000 (1995).
- ¹³I. Bertini and C. Luchinat, *Coord. Chem. Rev.* **150**, 1 (1996).
- ¹⁴D. J. Brown, M. Gerloch, and J. Lewis, *Nature (London)* **220**, 256 (1968).
- ¹⁵GAUSSIAN 94, Revision B.3, M. J. Frisch, G. W. Trucks, H. B. Schlegel, P. M. W. Gill, B. G. Johnson, M. A. Robb, J. R. Cheeseman, T. Keith, G. A. Petersson, J. A. Montgomery, K. Raghavachari, M. A. Al-Laham, V. G. Zakrzewski, J. V. Ortiz, J. B. Foresman, C. Y. Peng, P. Y. Ayala, W. Chen, M. W. Wong, J. L. Andres, E. S. Replogle, R. Gomperts, R. L. Martin, D. J. Fox, J. S. Binkley, D. J. Defrees, J. Baker, J. P. Stewart, M. Head-Gordon, C. Gonzalez, and J. A. Pople, Gaussian, Inc., Pittsburgh, PA, 1995.
- ¹⁶R. Poirier, R. Kari, and I. G. Csizmadia, *Handbook of Gaussian Basis Sets* (Elsevier, Amsterdam, 1985); the Mn basis set used is #25.11.3, p. 539, augmented by an extra Mn(3d) function with exponent 0.1054.
- ¹⁷J. B. Ellern and R. O. Ragsdale, *Inorganic Syntheses*, edited by W. L. Jolly (McGraw-Hill, New York, 1968), Vol. 11, pp. 82–84.
- ¹⁸H. F. Holtzclaw and J. P. Collman, *J. Am. Chem. Soc.* **79**, 3318 (1957).
- ¹⁹B. N. Figgis and J. Lewis, *Modern Coordination Chemistry*, edited by J. Lewis and R. G. Wilkins (Interscience Publishers, New York, 1960), pp. 400–454.